Methane Adsorption Characteristics of HKUST-1 and MIL-101(Cr) using GCMC (Grand Canonical Monte Carlo) Simulation

Teo, How Wei Benjamin
School of Mechanical and Aerospace Engineering, Nanyang Technological University

Chakraborty, Anutosh
School of Mechanical and Aerospace Engineering, Nanyang Technological University

KYUSHU UNIVERSITY

Methane Adsorption Characteristics of HKUST-1 and MIL-101(Cr) using GCMC (Grand Canonical Monte Carlo) Simulation

How Wei Benjamin Teo, Anutosh Chakraborty[*]

School of Mechanical and Aerospace Engineering, Nanyang Technological University,
50 Nanyang Avenue, Singapore 639798

*Author to whom correspondence should be addressed,
E-mail: AChakraborty@ntu.edu.sg

HKUST-1 and MIL-101 are undergone numerous gas storage experiments. In this paper, both MOFs are tested with methane adsorption employing grand canonical monte carlo (GCMC) simulation for the temperatures of 80K, 85K, 130K, 160K 240K and 298K to understand the behaviors of CH_4 molecules on MOF pores. We have found that MIL-101 shows the maximum uptake of 40 mol/kg at 80K. However, HKUST-1 reaches saturation uptake at pressure much lower than MIL-101 at all temperatures. The heats of adsorption (Q_{st}) are calculated at zero surface coverage for both adsorbent materials employing GCMC simulation, and HKUST-1 provides the higher values than the Q_{st} of MIL-101. The molecular modeling shows that MIL-101 adsorbents have excellent methane sorption at 80K. With these simulated results, the focus on improving methane adsorption by changing the adsorbent structure can be further narrowed down.

1. Introduction

The escalating threat of global warming due to harmful emissions of greenhouse gases has put the interests in clean energy research. Natural gas consisting mainly of methane (CH_4) has the potential to replace the existing hydrocarbon-based fuel such as petroleum due to its maximum hydrogen to carbon ratio. The use of CH_4 results in lower release of CO and CO_2 per unit of energy generation [1]. In addition, natural gas also provides lower SOx and NOx emissions [2]. However, the wide-spread use of the CH_4 is limited to its low energy density and the consequent necessity of its storage either at very high pressure or as a liquefied natural gas [3]. The transportation of natural gas is generally conducted in its liquid form. Conventionally, there are three different ways of natural gas storage namely (i) the compressed natural gas (CNG), (ii) the liquefied natural gas (LNG), and (iii) the adsorbed natural gas (ANG). For example, the use of CNG is limited to costly multi-stage gas compressors which consume high energy and require weighty, large fuel tanks [4]. The use of LNG is limited to the difficulties of handling a cryogenic fuel [5]. As an alternative to LNG and CNG, the ANG system can be designed with porous adsorbents to store NG at relatively low pressure that would permit light-weight fuel tanks which would be optimally incorporated into the limited space [6]. The US Department of Energy (DOE) has fixed CH_4 storage targets for adsorbents at 350 cm^3 CH_4 (STP) per cm^3 adsorbent and 0.5 g CH_4 per g of adsorbent at ambient conditions [4].

Currently, a new class of microporous material namely Metal Organic Frameworks (MOFs) [7-10] has been drawn attention for the storage of methane at room temperature and 35 bar due to their designable and high micro-porosity. These materials are made by the self-assembly of organic ligands and metal-containing nodes. MIL-101(Cr) (MIL, Matérial Institut Lavoisier), a crystalline mesoporous material, designed by Férey et al., [11] is a Cr terephthalate with inner free-cage diameter of up to 34Å. HKUST, a Cu(BTC) structure with cage diameter of 18Å, was created by Chui et al.[12] Both materials have been experimented with different types of gas sorption with results that are useful for certain adsorption applications [13-16].

In this paper, the MOF structures undergo methane adsorption using GCMC simulation to ease the process of understanding the behavior of the materials with methane adsorption. Methane adsorption isotherms are simulated and compared below the triple point temperature to analyse its sorption capabilities below its solid phase pressure. The simulated results provides a direction on how the adsorbents could be further modified for better adsorption behavior, by changing the structure of the adsorbent using Post-Synthesis Modification techniques [17].

2. Methodology

Multipurpose Simulation Code, also known as MuSiC,[18] will be used to run the GCMC simulation for the Methane adsorption with the HKUST-1 and MIL-101. Both adsorbents will undergo methane adsorption at six temperatures. These six temperatures will be classified into three categories: below triple point temperature region (80K and 85K), low temperature region (130K and 160K) and high temperature region (240K and 298K).

With methane as a non-polar molecule, methane adsorption to the MOFs will be solely based on van der Waals interactions. Thus, the interaction of methane molecules with the MOFs will be achieved using 12-6 Lennard Jones (LJ) potential. In MuSiC, methane is recognized as a single atom. The solid – fluid collision diameter (σ) and the depth of the solid – fluid potential well (ε) will be calculated based on UFF force field.[19] Lorentz – Berthelot mixing rules will be used for cross interaction of different atoms with the following equations [20]

$$\phi_{ij} = 4\varepsilon_{ij}\left[\left(\frac{\sigma_{ij}}{r_{ij}}\right)^{12} - \left(\frac{\sigma_{ij}}{r_{ij}}\right)^{6}\right] \qquad (1)$$

$$\sigma_{ij} = \frac{1}{2}(\sigma_i - \sigma_j) \qquad (2)$$

$$\varepsilon_{ij} = \sqrt{\varepsilon_i \varepsilon_j} \qquad (3)$$

where ϕ represents the adsorbent – adsorbate interaction potential and r defines the distance between a site of molecule i and a site of molecule j. Table 1 shows the σ and ε of methane and the interaction atoms of methane with HKUST-1 and MIL-101 using Lorentz – Berthelot mixing rules equation.

Table 1: σ and ε for methane, MIL-101 and HKUST-1.

Atoms	σ(Å)	ε(K)
Methane	3.73	148
Methane-Carbon(HKUST-1 & MIL-101)	3.58	88.431
Methane-Oxygen(HKUST-1 & MIL-101)	3.424	66.848
Methane-Chromium(MIL-101)	3.212	33.424
Methane-Hydrogen(HKUST-1)	3.151	57.245
Methane-Copper(HKUST-1)	3.422	19.297

3. Result and Discussion

The triple point temperature for methane is 90.7K. By running the simulation at 80K and 85K, simulation may be running an adsorption process with a solid – liquid state adsorbate. Figure 1 illustrates the adsorption isotherms of each MOF at 80K and 85K. MIL-101 has better uptake as compared to HKUST-1. At 80K, MIL-101 has a significant increase in uptake at a low pressure up to 2.1kPa, where the uptake is about 40 mol/kg of adsorbent. At 85K, the uptake is not as high as that at 80K before reaching the pressure of 2.1kPa. The isotherms have no results after 2.1kPa and 4.9kPa for 80K and 85K respectively. This may due to working pressure is above the solid – gaseous boundary, hence, methane is in solid state. On the other hand, the isotherms for HKUST-1 show the uptake of about 21mol/kg at 80K and 1kPa. Literatures state that the smaller pores have deep potential well [16, 21] and contributes strong adsorption field. Thus, adsorption occurs at lower pressure for HKUST-1. Further experiment for adsorption at this temperature range is necessary to verify these simulated results.
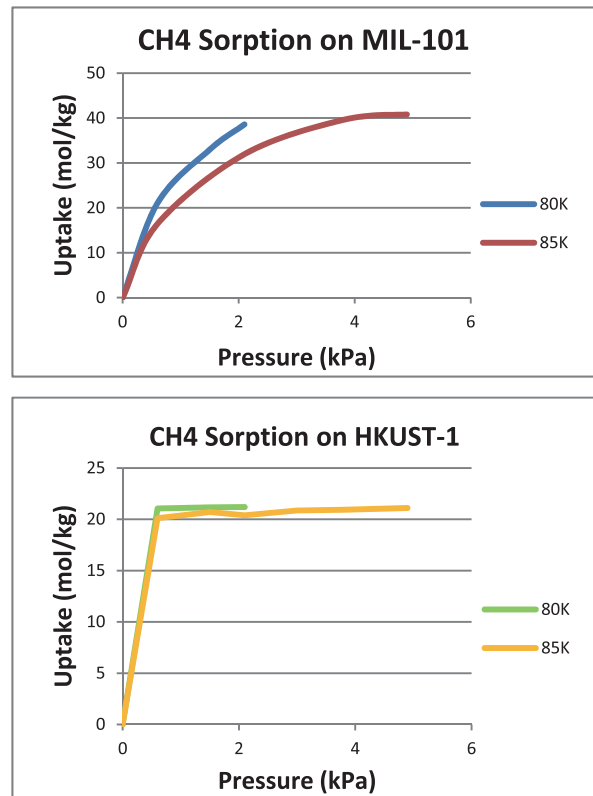

Figure 1: Adsorption Isotherms of MIL-101 and HKUST-1 at 80K and 85K

At low temperature region, methane is in its gaseous state as the temperature region passes the boiling point temperature of methane. Figure 2 shows the adsorption isotherms at 130K and 160K. The maximum uptake of each individual MOF slightly decreases at 130K as compared to those in Figure 1. The difference between the isotherms and those in Figure 1 is the pressure required for uptake to reach its maximum is higher as temperature increases. This is due to desorption at a relatively higher temperature. After 367.9kPa, isotherms have no results of methane sorption uptake due to the change of phase of methane to saturated liquid.
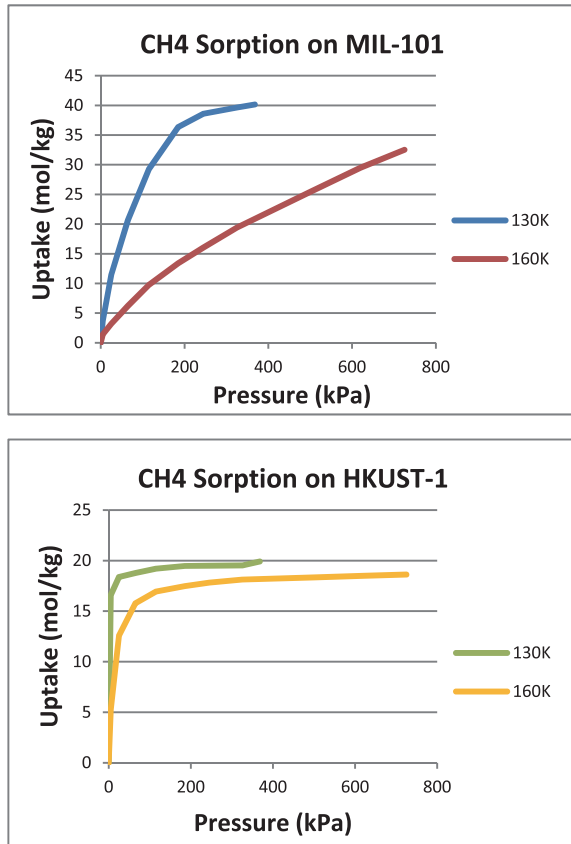

Figure 2: Adsorption Isotherms of MIL-101 and HKUST-1 at 130K and 160K

At 160K, adsorption isotherm for MIL-101 increases more linearly as compared to 130K. Adsorption isotherm for HKUST-1 is able to reach saturation at lower pressure. Figure 3 shows the adsorption isotherms of the MOFs at high temperature region. Similarly, the isotherms on MIL-101 are getting linear as temperature increases. The adsorbed amount also decreases as the temperature increases. The decrement of adsorbed amount is also observed at the isotherms on HKUST-1, but the isotherms are able to reach saturation uptake at lower pressure as compared to MIL-101.
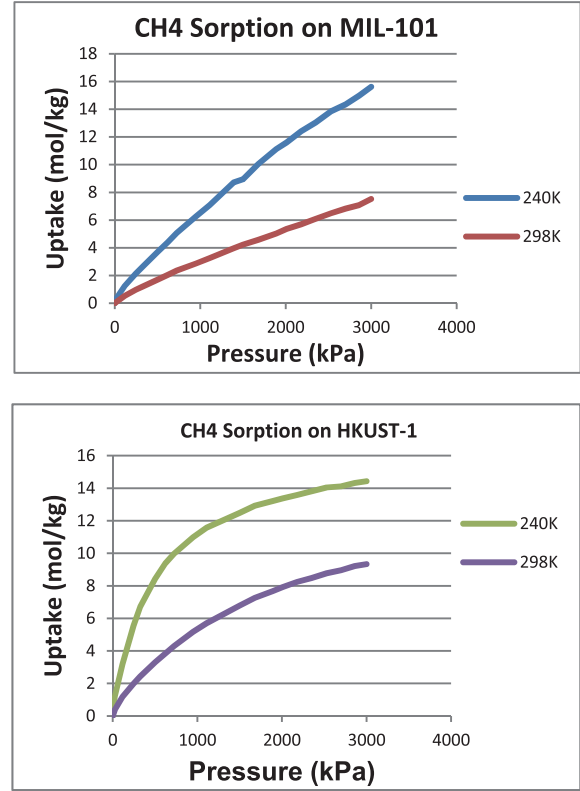

Figure 3: Adsorption Isotherms of MIL-101 and HKUST-1 at 240K and 298K

As mention above, the decrement of the adsorbed amount as temperature increases is due to desorption taking place at a relatively high temperature. This is agreeable as other sorption experiments have encountered the same behavior with these MOFs [16, 22]. It is noted that MIL-101 has larger pore size as compared to HKUST-1. This would probably explain the high uptake saturation for MIL-101. As mentioned, given that smaller pores have deep potential well and this contributes strong adsorption field. Hence, a smaller pore MOF, like HKUST-1, adsorbs more gas at lower pressure [16, 21], which explains the fact that MIL-101 isotherms are more linear as temperature increases.

To further support the simulated results, the average isosteric heat of adsorption, Q_{st}, for each MOF at different working temperature is calculated. The following equation is used to calculate the average isosteric heat of adsorption [23, 24]:

$$Q_{st} = RT - \left(\frac{\partial \langle v \rangle}{\partial \langle x \rangle}\right)_T \qquad (4)$$

where $\langle v \rangle$ is the potential average of adsorbed phase and $\langle x \rangle$ is the uptake amount average at temperature T. R is the universal gas constant. Table 2 shows the isosteric heat of adsorption of HKUST-1 and MIL-101 based on the simulated results.

- 46 -

Table 2: Average Isoteric Heat of Adsorption for HKUST-1 and MIL-101

Temperature (K)	Q_{st} for HKUST-1 (kJ/mol)	Q_{st} for MIL-101 (kJ/mol)
80	8.22712	3.25072
85	8.66719	2.88
130	8.976	4.597
160	10.5862	6.1315
240	12.529	9.218
298	13.594	9.739
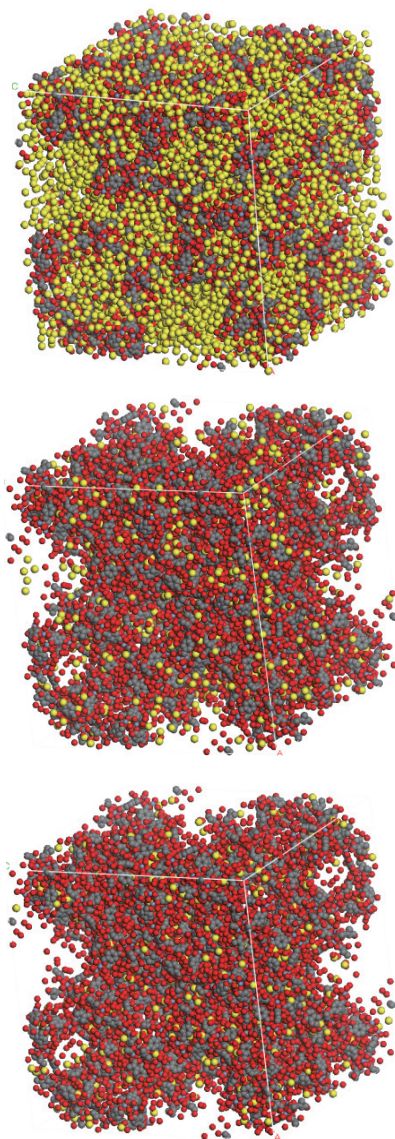
Figure 4: Methane Adsorption on MIL-101 structures at 80K(top), 130K(middle) and 298K(bottom)

The average isosteric heat of adsorption at HKUST-1 is higher than MIL-101 for all the temperature tested for methane sorption simulation. This study clearly shows that HKUST-1 perform better than MIL-101 in terms of methane adsorption regardless of the uptake amount at saturation conditions.

Using the results from the simulation, a molecular modeling of methane adsorption on the MOF structures are shown in Figure 4. Methane adsorption at 80K with a pressure of 4kPa on MIL-101 is tremendously high as compared to those at higher temperature. As the results are based on simulation, further experiment is required to prove the authentication of the simulated results.

4. Conclusions

Methane adsorption was performed on HKUST-1 and MIL-101 using GCMC simulation. Comparing the adsorption isotherms at 80K, MIL-101 has the uptake of 40mol/kg, which is twice of that of HKUST-1. This is probably due to the large pore size of MIL-101. However, HKUST-1 is able to reach its saturation uptake at lower pressure at all temperatures comparing to MIL-101. As temperature increases, isotherms of MIL-101 tend to be linear and higher pressure is required for saturation to take place. As HKUST-1 has smaller pores, it is able to adsorb more gas at lower pressure. Isoteric heat of adsorption for both MOFs were calculated and it is shown that the Q_{st} for HKUST-1 were higher than those of MIL-101. Molecular modeling of methane adsorption showed that MIL-101 can adsorb higher number of methane molecules at 80K as compared to other temperatures. Experiment regarding methane adsorption at triple point temperature is highly recommended to certify the results achieved by GCMC simulation. These simulated results provide sufficient information on the direction to improve methane adsorption on MOF.

References

1) Y. He, W. Zhou, G. Qian, and B. Chen, "Methane storage in metal-organic frameworks," *Chemical Society Reviews,* vol. **43**, pp. 5657-5678, 2014.

2) R. S. Middleton and J. K. Eccles, "The complex future of CO_2 capture and storage: Variable electricity generation and fossil fuel power," *Applied Energy,* vol. **108**, pp. 66-73, 2013.

3) M. G. Waller, E. D. Williams, S. W. Matteson, and T. A. Trabold, "Current and theoretical maximum well-to-wheels exergy efficiency of options to power vehicles with natural gas," *Applied Energy,* vol. **127**, pp. 55-63, 2014.

4) J. A. Mason, M. Veenstra, and J. R. Long,

"Evaluating metal–organic frameworks for natural gas storage," *Chem. Sci.,* vol. **5**, pp. 32-51, 2014.

5) M. Miana, R. d. Hoyo, V. Rodrigálvarez, J. R. Valdés, and R. Llorens, "Calculation models for prediction of Liquefied Natural Gas (LNG) ageing during ship transportation," *Applied Energy,* vol. **87**, pp. 1687-1700, 2010.

6) J. Wegrzyn and M. Gurevich, "Adsorbent Storage of Natural Gas," *Applied Energy,* vol. **55**, pp. 71-83, 1996.

7) S. Bauer, C. Serre, T. Devic, P. Horcajada, J. Marrot, G. Ferey*, et al.*, "High-throughput assisted rationalization of the formation of metal organic frameworks in the iron(III) aminoterephthalate solvothermal system," *Inorganic Chemistry,* 2008.

8) H. Furukawa, F. Gandara, Y. B. Zhang, J. Jiang, W. L. Queen, M. R. Hudson*, et al.*, "Water adsorption in porous metal-organic frameworks and related materials," *J Am Chem Soc,* vol. **136**, pp. 4369-81, Mar 19 2014.

9) O. V. Gutov, W. Bury, D. A. Gomez-Gualdron, V. Krungleviciute, D. Fairen-Jimenez, J. E. Mondloch*, et al.*, "Water-stable zirconium-based metal-organic framework material with high-surface area and gas-storage capacities," *Chemistry,* vol. **20**, pp. 12389-93, Sep 22 2014.

10) F. Jeremias, A. Khutia, S. K. Henninger, and C. Janiak, "MIL-100(Al, Fe) as water adsorbents for heat transformation purposes—a promising application," *Journal of Materials Chemistry,* vol. **22**, p. 10148, 2012.

11) G. Ferey, C. Mellot-Draznieks, C. Serre, F. Millange, J. Dutour, S. Surble*, et al.*, "A chromium terephthalate-based solid with unusually large pore volumes and surface area," *Science,* vol. **309**, pp. 2040-2042, Sep 23 2005.

12) S. S. Y. Chui, S. M. F. Lo, J. P. H. Charmant, A. G. Orpen, and I. D. Williams, "A Chemically Functionalizable Nanoporous Material [Cu3(TMA)2(H2O)3]n," *Science,* vol. **283**, pp. 1148-1150, 1999.

13) J. Ehrenmann, S. K. Henninger, and C. Janiak, "Water Adsorption Characteristics of MIL-101 for Heat-Transformation Applications of MOFs," *European Journal of Inorganic Chemistry,* vol. **2011**, pp. 471-474, 2011.

14) E. N. F. Gul, B. Jee, A. Poppl, M. Hartmann, D. Himsl, and M. Bertmer, "Effects of varying water adsorption on a Cu3(BTC)2 metal-organic framework (MOF) as studied by 1H and 13C solid-state NMR spectroscopy," *Phys Chem Chem Phys,* vol. **13**, pp. 7783-8, May 7 2011.

15) A. Khutia, H. U. Rammelberg, T. Schmidt, S. Henninger, and C. Janiak, "Water Sorption Cycle Measurements on Functionalized MIL-101Cr for Heat Transformation Application," *Chemistry of Materials,* vol. **25**, pp. 790-798, 2013.

16) S. Ye, X. Jiang, L.-W. Ruan, B. Liu, Y.-M. Wang, J.-F. Zhu*, et al.*, "Post-combustion CO2 capture with the HKUST-1 and MIL-101(Cr) metal–organic frameworks: Adsorption, separation and regeneration investigations," *Microporous and Mesoporous Materials,* vol. **179**, pp. 191-197, 2013.

17) Z. Wang and S. M. Cohen, "Postsynthetic modification of metal-organic frameworks," *Chem Soc Rev,* vol. **38**, pp. 1315-29, May 2009.

18) A. Gupta, S. Chempath, M. J. Sanborn, L. A. Clark, and R. Q. Snurr, "Object-oriented Programming Paradigms for Molecular Modeling," *Molecular Simulation,* vol. **29**, pp. 29-46, 2003.

19) A. K. Rappé, C. J. Casewit, K. S. Cowell, W. A. Goddard, and W. M. Skiff, "UFF, a Full Periodic Table Force Field for Molecular Mechanics and Molecular Dynamics Simulations," *J Am Chem Soc,* vol. **114**, pp. 10024-10035, 1992.

20) I. Kühn, "A Generalized Potential Theory of Adsorption I. The Derviation of a General Equation for Adsorption Isotherms," *Journal of Colloid and Interface Science,* vol. **23**, pp. 563-571, 1967.

21) L. Huang, L. Zhang, Q. Shao, L. Lu, X. Lu, S. Jiang*, et al.*, "Simulation of Binary Mixture Adsorption of Carbon Dioxide and Methane in Carbon Nanotube: Temperature, Pressure, and Pore Size Effects," *Journal of Physical Chemistry C,* vol. **111**, pp. 11912-11920, 2007.

22) P. Chowdhury, S. Mekala, F. Dreisbach, and S.

Gumma, "Adsorption of CO, CO2 and CH4 on Cu-BTC and MIL-101 metal organic frameworks: Effect of open metal sites and adsorbate polarity," *Microporous and Mesoporous Materials,* vol. **152**, pp. 246-252, 2012.

23) P. L. Llewellyn, S. Bourrelly, C. Serre, A. Vimont, M. Daturi, L. Hamon*, et al.*, "High uptakes of CO2 and CH4 in mesoporous metal-organic frameworks MIL-100 and MIL-101," *Langmuir,* vol. **24**, pp. 7245-7250, 2008.

24) H. Guo, F. Shi, Z. Ma, and X. Liu, "Molecular Simulation for Adsorption and Separation of CH_4/H_2 in Zeolitic Imidazolate Frameworks," *J. Phys. Chem. C,* vol. **114**, pp. 12158-12165, 2010.

25) R. Q. Snurr, A. T. Bell, and D. N. Theodorou, "Prediction of Adsorption of Aromatic Hydrocarbons in Silicalite from Grand Canonical Monte Carlo Simulations with Biased Insertions," *The Journal of Physical Chemistry,* vol. **97**, pp. 13742-13752, 1993.